Journal of Theoretical Biology 610 (2025) 112145

Contents lists available at ScienceDirect

Journal of Theoretical Biology

journal homepage: www.elsevier.com/locate/jtbi

# Heat delivery accompanying pulsed field ablation

Angiolo Farina [a,*], Antonio Fasano [b], Massimo Grimaldi [c,d], Fabio Rosso [a]

[a] Dipartimento di Matematica e Informatica "Ulisse Dini", Viale Morgagni 67/a, Firenze, 50134, Italy
[b] Fiab SpA, Via Bruno Passerini, 2, Vicchio (FI), 50039, Italy
[c] Ospedale "F. Miulli", Acquaviva delle Fonti, Bari, 70021, Italy
[d] Dipartimento di Medicina, Università LUM, Casamassima, Bari, 70010, Italy

ARTICLE INFO

*Keywords:*
Pulsed field ablation (PFA)
Atrial fibrillation (AF)
Esophageal thermal lesion (ETL)
Mathematical modeling
Heat diffusion
Joule effect

ABSTRACT

Pulsed Field Ablation (PFA) is a technique to achieve pulmonary vein isolation, alternative to the traditional thermal ablation procedures. Instead of delivering or subtracting heat, PFA uses rapid pulses of a high intensity electric field, inducing cells electroporation. PFA is usually claimed not to influence the temperature in the surroundings of the ablation site. Nevertheless, in some case a non-negligible increase of the patient's luminal esophageal temperature has been observed. Here we set up a mathematical model to provide a theoretical basis to the latter observation, considering a worst case scenario.

## 1. Introduction: Pulsed field ablation and thermal considerations

Pulsed Field Ablation (PFA) is an emerging technique in the treatment of atrial fibrillation (AF), offering a novel approach to tissue ablation through the mechanism of irreversible electroporation (IRE) (see, e.g., Verma et al., 2022; Badertscher et al., 2025; Kirstein et al., 2024; Farnir et al., 2025; Deering et al., 2024; Tang et al., 2024). Unlike traditional thermal-based methods such as radiofrequency (RF) or cryoablation (see, e.g., Shehadeh et al., 2024), which rely on heating or freezing to destroy cardiomyocytes, PFA employs high-intensity pulsed electric fields to selectively disrupt cell membranes. This targeted action is attributed to the lower damage threshold of cardiomyocytes compared to other cell types (see Fig. 1a). In vivo animal studies confirm that PFA is able to determine welldefined myocardial lesions while maintaining intact vascular and nervous structures (Grimaldi et al., 2022). Despite its characterization as a non-thermal modality, the term *non-thermal* should not be interpreted literally. Actually, in some cases a non-negligible increase at the luminal esophageal temperature has been reported (Kirstein et al., 2024). The delivery of intense electrical pulses results in localized Joule heating, especially in the vicinity of the electrodes. Although mechanisms like heat diffusion and blood flow are such to mitigate temperature increase at a distance, the thermal aspect of PFA must be thoroughly evaluated (see, e.g., Yoo and Heist, 2024; Cho et al., 2024; Shehadeh et al., 2024) to ensure procedural safety and avoid complications like esophageal thermal lesion (ETL), a significant risk in thermal ablation procedures. Indeed, the exposure to an excessive thermal field can result into an atrio-esophageal fistula, a catastrophic outcome (see Shehadeh et al., 2024). It is important to emphasize that RF ablation procedures also entail inherent risks, as previously discussed in (Farina et al., 2024).

To the best of our knowledge, apart from the aforementioned paper by Kirstein et al. (2024), and a very recent contribution by Kocharian et al. (2025), no experimental data exist regarding the thermal effects of PFA. The objective of this paper is to draw attention to this relatively unexplored topic by investigating the thermal dynamics of PFA. Specifically, we aim to:

a) Quantify heat production: derive estimates of heat generated near the electrodes during PFA procedures.
b) Model heat diffusion: develop a mathematical model to predict the evolution of the temperature field in surrounding tissues, including the esophagus.
c) Assess safety: provide a framework for assessing thermal risks associated with PFA.

To achieve these objectives, the study employs an idealized geometric model to simplify the complexities of patient anatomy while capturing the essential physics of heat generation and transfer. By focusing on order-of-magnitude estimates and key parameters (e.g., pulse intensity, tissues conductivity, and heart pulse period), the work provides insights into the thermal effects of PFA accounting for the observation of Kirstein et al. (2024), reporting a 5K increase of the luminal esophageal temperature (see also Pearce, 2013).

This exploration is particularly relevant as the adoption of PFA is growing fast, necessitating a deeper understanding of its implications to refine procedural protocols and enhance patient safety.

* Corresponding author.
*E-mail addresses:* angiolo.farina@unifi.it (A. Farina), a.fasano@fiab.it (A. Fasano), m.grimaldi@miulli.it (M. Grimaldi), fabio.rosso@unifi.it (F. Rosso).

https://doi.org/10.1016/j.jtbi.2025.112145
Received 28 February 2025; Received in revised form 8 May 2025; Accepted 14 May 2025
Available online 22 May 2025

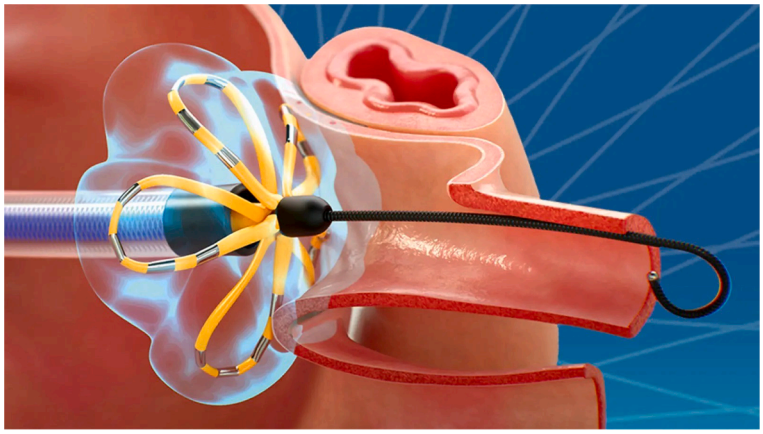

**(a).** The electrical device (introduced through the femoral vein) reaches the pulmonary vein ostium facing the atrium. Periodic high voltage currents are generated for extremely short time intervals.

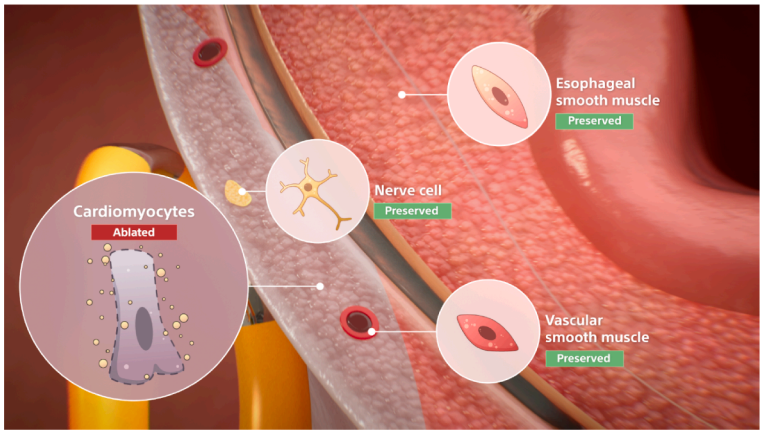


**(b).** The applied high voltage induces the irreversible electroporation (IRE) of cardiomyocytes of cardiac tissue preserving other local cells and muscles.

**Fig. 1.** FARAPULSE™ pulsed field ablation system (both images are copyrighted and are reproduced under permission by Boston Scientific Co.).

## 2. The physical problem

In this section, we illustrate the physical problem and the corresponding mathematical model. We consider a bipolar PFA ablator, which typically consists of an array of electrodes in contact with a pulmonary vein ostium (see Fig. 1a). The typical length of an electrode is $h = 2\,\text{mm}$, and this is also the distance between two consecutive electrodes (a detailed description of the PFA procedure can be found, e.g., in Badertscher et al., 2025; Reddy et al., 2019; de Asmundis and Chierchia, 2021, while for a comparison of PFA with other techniques for the treatment of AF, we refer to Rattka et al., 2024).

Fig. 2 shows a schematic representation of the PFA ablator with the electrodes and the pulsed currents (grey regions) generated between each pair.

We assume these currents are concentrated in a spherical region of diameter $h$. In reality, the currents flow through an oval-shaped region, whose determination is computationally complex. In the model we assume that currents flow uniformly through the above said spherical regions between consecutive electrodes. Such an approximation largely simplifies computation without significantly affecting the results.

The applied voltage $V(t)$ consists of a series of $N$ biphasic pulses (i.e. alternating in polarity), typically $N = 5$. Each pulse has a peak amplitude $V_{\max}$ on the order $\sim 10^3$ V (typically 2000 V), and a duration $t_p$ ranging from hundreds of microseconds to milliseconds. These pulses are repeated with a period $\tau_p$ of approximately 0.5 s, resulting in a single application duration of about 2–3 s per cycle (see Fig. 3). Each application is repeated $\mathcal{N}_{\text{app}}$ times per vein (typically $\mathcal{N}_{\text{app}} = 8$, see Rattka et al. (2024)), alternating between two catheter configurations: four applications in the *flower* configuration and four in the *basket* configuration. The catheter was repositioned and/or rotated every two applications to optimize coverage ot the target issue.

The time interval $\Delta$ between successive applications is of the order of seconds or longer to allow for precise catheter positioning. This is necessary to ensure optimal circumferential coverage of the pulmonary vein ostium and antral regions based on PV angiography. For instance, assuming $\Delta = 5$ s, the total procedure time for a single vein would be approximately 60 s.

Due to the linearity of the heat equation, the evolution of the thermal field can be modeled as the superposition of $\mathcal{N}_{\text{app}}$ (e.g., eight) single applications, each lasting 2–3 s and temporally shifted by a time interval $\Delta$.

The model that we will illustrate below to determine the temperature of the tissue surrounding the PF ablator is based on the clear separation between the time scale of heat diffusion and that characterizing the electric power delivery. We will therefore first consider the heating phase caused by the Joule effect, which essentially only affects the areas through which the current flows. Once these regions have warmed up (which in practice happens instantaneously with respect to the diffusion time scale), we will analyze how the heat spreads through the tissue possibly reaching sensitive areas such as the esophagus.

The heating phase must be carefully modeled. In fact, about half of the sphere crossed by the electric current is occupied by the blood that is

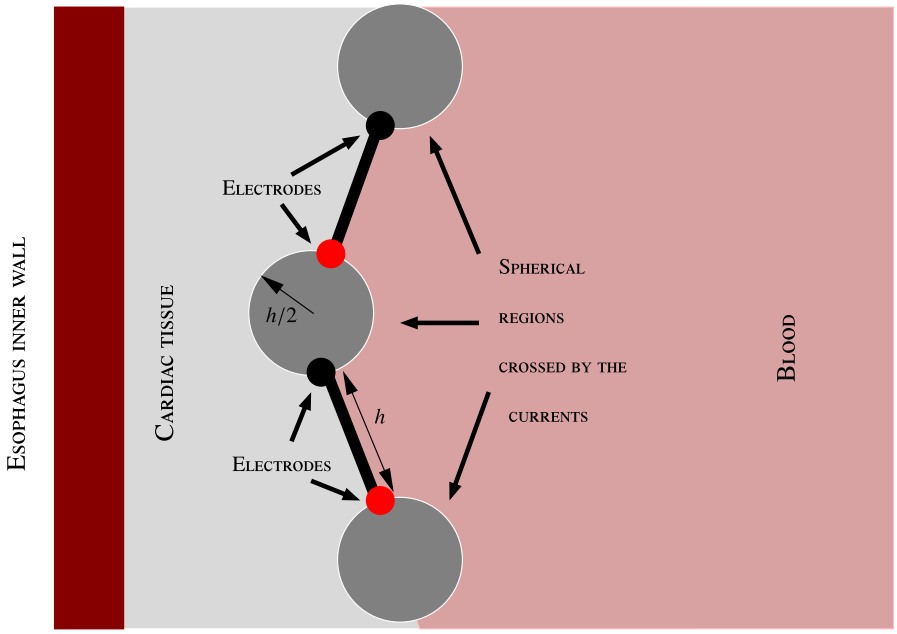


**Fig. 2.** Scheme of electrodes and currents. Such a section is supposed to face the esophagus in a worst case scenario ($h \approx 2$mm).

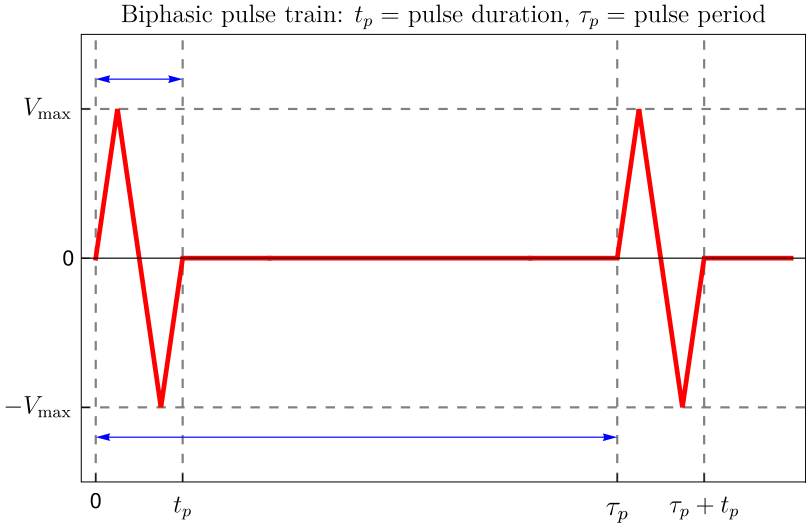


**Fig. 3.** Biphasic periodic pulse of period $\tau_p$. The electrical pulse has a duration $t_p$ which is significantly less than the period $\tau_p$ with which the pulses are repeated (figure scale is exaggerated for visualization purposes).

in the atrium and is replaced with the period $\tau_b \approx 1$ s. Therefore, at each heartbeat, blood at body temperature comes into contact with the tissue heated by the Joule effect, thus removing some of the heat accumulated.

## 3. Time scales involved in PFA

A crucial step for modeling the heat delivery during PFA is to compare the various time scales involved in the process. The following time scales are relevant to the phenomenon under investigation:

- The period $\tau_p$ of the pulse. Typically $\tau_p \approx 0.5$ s.
- The duration $t_p$ of the high voltage application. Typically $t_p$ ranges between $10^{-4}$s and $10^{-3}$s. Shorter values are also possible, but here we are interest to emphasize what happens in the worst scenario and the model is calibrated accordingly.
- The application time $\tau_a$. If $\nu$ heartbeats occur in a single application, then, for the sake of simplicity, we set $\tau_a = \nu\tau_b$. Typically $\nu = 3$ and so $\tau_a \approx 3$ s.
- The heating time $t_w$. We define $t_w$ as the time needed to raise the temperature of the sphere of radius $h$ by $\vartheta_c = 1$ K, above the basal temperature when it receives the power pulse. We shall see in the sequel that $t_w = O(10^{-5})$ s.
- The heat diffusion characteristic time $t_d$ in the body. We shall see in the sequel that $t_w = O(10)$ s.
- The blood replacement time period $\tau_b$. Blood is replaced in the atrium at each heartbeat. Thus $\tau_b \approx 1$ s. In PFA treatments $\tau_p < \tau_b$, and we write $\tau_b = n\tau_p$. Typically $n = 2$. In practice, we may assume that the blood in the hemisphere heats up by receiving two pulses (whose individual duration is $t_p$). After being replaced in the atrium, the blood in the hemisphere facing the tissue starts to warm up again as it is crossed by the current pulses.

Let us estimate both $t_w$ and $t_d$. Concerning $t_w$ we have

$$\varrho c V_{el}\, \vartheta_c = W t_w \tag{1}$$

where $V_{el} = \frac{4}{3}\pi\left(\frac{h}{2}\right)^3$ is the volume of the sphere, $W$ the electrical power dissipated in it, $\varrho$ is density and $c$ is the specific heat. Typical values are $\varrho = 1.5 \cdot 10^3\ \mathrm{kgm^{-3}}$, and $c = 3.7 \cdot 10^3\ \mathrm{J\,m^{-3}K^{-1}}$. The electrical power dissipated in the sphere during the pulse is given by $W = \langle V^2 \rangle / Z$, where

$$\langle V^2 \rangle = \frac{1}{t_p}\int_0^{t_p} V^2(t)dt = \frac{V_{\max}^2}{3}, \tag{2}$$

with $Z$ the electric resistance and $V(t)$ the applied voltage represented in Fig. 3. The resistance $Z$ is estimated replacing the sphere with a cylinder of same volume and height $h$, thus with a radius $R_c = h/\sqrt{6}$. Hence

$$Z = \frac{h}{\sigma\pi R_c^2} = \frac{6}{\pi\sigma h}, \tag{3}$$

where $\sigma$ denotes the medium electric conductivity (typically $\sigma = 1\ \mathrm{S\ m^{-1}}$, Peters et al., 2001) which we suppose to be homogeneous. We thus have

$$W = \pi\sigma h V_{\max}^2/18, \tag{4}$$

and therefore definition (1) gives

$$t_w = 3\frac{\varrho c h^2}{\sigma V_{\max}^2}\,\vartheta_c. \tag{5}$$

In particular, if $\vartheta_c = 1$ K, then $t_w \sim 67\ \mu$s.

Concerning $t_d$, we are interested in the time needed by the heat to travel, by diffusion, to a distance comparable to the radius of the region hit by the current, i.e. $h$. We thus have

$$t_d = \frac{\varrho c h^2}{k}, \tag{6}$$

where $k$ is the thermal conductivity. Since a typical value for the thermal conductivity of living tissues is $k = 0.5\ \mathrm{Wm^{-1}K^{-1}}$ , we obtain $t_d \sim 40$ s.

We conclude that

$$t_w \lesssim t_p \ll \tau_p < \tau_b < \tau_a \ll t_d$$

The main consequence of the facts just established is that the power delivered in a pulse is essentially used to uniformly heat up the sphere crossed by the current since diffusion will take a much longer time to take heat away. On the other hand blood is replaced in half of the sphere with a period $\tau_b < \tau_a$. Consequently at regular intervals (period $\tau_b$) the temperature of half of the sphere crossed by the current is brought back to the basal temperature, thus contributing to cooling the other half of the sphere occupied by the tissue. At the end of a single application (which is practically instantaneous in terms of the $t_d$ scale), the hemisphere occupied by the tissue has a higher temperature than the basal one. We therefore model the heating process accompanying the PFA treatment as a two-stage process:

- In the first stage (power delivering stage) the tissue crossed by the current is uniformly heated by the Joule effect.
- In the second stage (diffusion stage) thermal diffusion comes into play, increasing the temperature of the areas close to the one crossed by the current.

## 4. Solid tissue and blood temperature rising during the power delivering stage (i.e. during a single application)

We denote by $\vartheta_B$ and by $\vartheta_T$ the temperature increase, with respect to basal level, experienced by the hemisphere in Fig. 4 occupied by blood and by the one occupied by the solid tissue, respectively.

Considering, for simplicity, the same density and specific heat for blood and tissue the evolution equation of $\vartheta_B$ and $\vartheta_T$ may be modeled as

$$\begin{cases} \frac{V_{el}}{2}\varrho c\,\frac{d\vartheta_B}{dt} = \frac{W}{2}\psi(t) - \pi\left(\frac{h}{2}\right)^2 S(\vartheta_B - \vartheta_T), \\ \frac{V_{el}}{2}\varrho c\,\frac{d\vartheta_T}{dt} = \frac{W}{2}\psi(t) - \pi\left(\frac{h}{2}\right)^2 S(\vartheta_T - \vartheta_B), \end{cases} \tag{7}$$

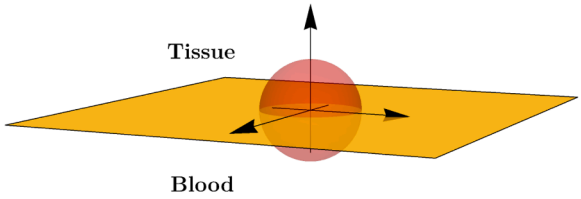


**Fig. 4.** The sphere of radius $h/2$ heated by the electric current. At the end of a single application, heat diffuses on both sides of the boundary tissue-blood.

where

$$\psi(t) = \begin{cases} 1, & \text{if } V(t) \neq 0, \\ 0 & \text{if } V(t) = 0, \end{cases}$$

and where the last terms in the equations represent the mutual heat exchange between tissue and blood, which is proportional to the contact area, namely $\pi\left(\frac{h}{2}\right)^2$. The coefficient $S$ (in $\mathrm{JK^{-1}m^{-2}s^{-1}}$) is the blood-tissue heat exchange coefficient. In the Appendix we illustrate the procedure for estimating it. Modeling the hemispheres temperature evolution by means of two ordinary differential equations makes sense due to their small dimensions.

It is convenient to introduce

$$\begin{cases} \vartheta_+ = \vartheta_T + \vartheta_B, \\ \vartheta_- = \vartheta_T - \vartheta_B, \end{cases} \quad \Leftrightarrow \quad \begin{cases} \vartheta_T = \frac{\vartheta_+ + \vartheta_-}{2}, \\ \vartheta_B = \frac{\vartheta_+ - \vartheta_-}{2}, \end{cases}$$

so that, recalling (1)–(3), and (5), we rewrite system (7) as

$$\begin{cases} \frac{d\vartheta_+}{dt} = 2\frac{\vartheta_c}{t_w}\psi(t), \\ \frac{d\vartheta_-}{dt} = -\frac{\vartheta_-}{t_m}, \end{cases} \tag{8}$$

where

$$t_m = \frac{\varrho c h}{6S}. \tag{9}$$

At the beginning of the power delivery, tissue and blood have the same temperature and therefore as initial conditions we take $\vartheta_B(0) = \vartheta_T(0) = 0$, i.e. $\vartheta_+(0) = \vartheta_-(0) = 0$. At $t = \tau_b \approx n\tau_p$, i.e. after two pulses (each of which has a duration $t_p$), we have $\vartheta_-(\tau_b) = 0$ and $\vartheta_+(\tau_b) = 2\vartheta_{\max}$, where, exploiting (5),

$$\vartheta_{\max} = \frac{nt_p}{t_w}\vartheta_c. \tag{10}$$

We thus conclude that two halves of the sphere have reached the same temperature $\vartheta_{\max}$. In particular, taking $\vartheta_c = 1$ K, which entails $t_w \sim 67\ \mu$s, and $n = 2$ (i.e. $\tau_p = 0.5$ s) we have $0.3\ \mathrm{K} \le \vartheta_{\max} \le 30\ \mathrm{K}$ when $t_p$ ranges between $10^{-4}$ s and $10^{-3}$ s.

After $n$ pulses, i.e. $t = \tau_b$, new blood, at basal temperature, enters the atrium and so the *new* initial conditions of system (7) have to be updated, namely

$$\vartheta_B(\tau_b) = 0, \quad \vartheta_T(\tau_b) = \vartheta_{\max},$$

which entail $\vartheta_+(\tau_b) = \vartheta_-(\tau_b) = \vartheta_{\max}$. After further $n$ power pulses have been delivered to the sphere, i.e. at time $t = 2\tau_b = 2n\tau_p$, we have

$$\vartheta_+(2\tau_b) = 3\vartheta_{\max}, \qquad \vartheta_-(2\tau_b) = \vartheta_{\max}\exp\left\{-\frac{n\tau_p}{t_m}\right\},$$

and so

$$\begin{aligned} \vartheta_T(2\tau_b) &= \frac{\vartheta_{\max}}{2}\left(3 + \exp\left\{-\frac{n\tau_p}{t_m}\right\}\right), \\ \vartheta_B(2\tau_b) &= \frac{\vartheta_{\max}}{2}\left(3 - \exp\left\{-\frac{n\tau_p}{t_m}\right\}\right). \end{aligned} \tag{11}$$

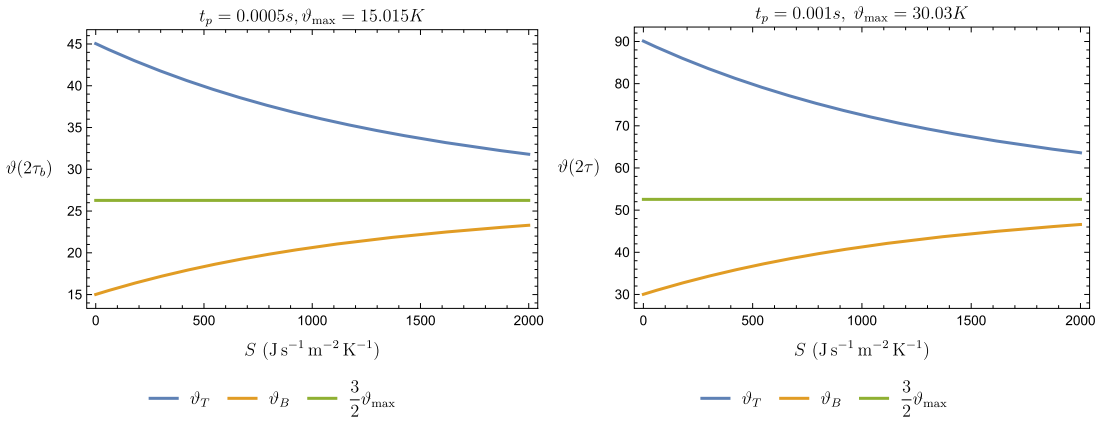


**Fig. 5.** Dependence of $\vartheta_T(2\tau_b)$ and $\vartheta_B(2\tau_b)$, given by (11), on the choice of $S$. The maximum of $\vartheta_T$ and the minimum of $\vartheta_B$, respectively, are attained when $S = 0$. On the other hand, when $S \to \infty$, $\vartheta_T$ and $\vartheta_B$ both converge to $3\vartheta_{\max}/2$. We notice that, because of (10), $\vartheta_{\max}$ depends significantly on the choice of $t_p$. On the left panel we show the case $t_p = 5 \times 10^{-4}$s, on the right panel the case $t_p = 10^{-3}$s.

We remark that, if $S = 0$, i.e. $1/t_m = 0$, (perfect thermal insulation between tissue and blood) we have $\vartheta_T(2\tau_b) = 2\vartheta_{\max}$ and $\vartheta_B(2\tau_b) = \vartheta_{\max}$ as expected. Conversely, if $S$ is very "large", i.e. $1/t_m \to \infty$ (perfect heat exchange between blood and tissue), then $\vartheta_T(2\tau_b)$ and $\vartheta_B(2\tau_b)$ both converge to $3\vartheta_{\max}/2$. Fig. 5 shows the behavior of $\vartheta_T(2\tau_b)$ and $\vartheta_B(2\tau_b)$ versus $S$.

The procedure is repeated at every $\tau_b$, that is, every $n$ pulses. For instance, at $t = 2\tau_b$, i.e. after two sets of $n$ pulses, the "new" initial conditions are

$$\vartheta_B(2\tau_b) = 0, \quad \vartheta_T(2\tau_b) = \frac{\vartheta_{\max}}{2}\left(3 + \exp\left\{-\frac{n\tau_p}{t_m}\right\}\right),$$

and at $t = 3\tau_b = 6n\tau_p$, we have

$$\vartheta_T(3\tau_b) = \vartheta_{\max}\left[1 + \frac{1}{4}\left(3 + \exp\left\{-\frac{n\tau_p}{t_m}\right\}\right)\left(1 + \exp\left\{-\frac{n\tau_p}{t_m}\right\}\right)\right],$$

$$\vartheta_B(3\tau_b) = \vartheta_{\max}\left[1 + \frac{1}{4}\left(3 + \exp\left\{-\frac{n\tau_p}{t_m}\right\}\right)\left(1 - \exp\left\{-\frac{n\tau_p}{t_m}\right\}\right)\right]. \tag{12}$$

Again, if $S = 0$, we have $\vartheta_T(3\tau_b) = 3\vartheta_{\max}$ and $\vartheta_B(3\tau_b) = \vartheta_{\max}$, while if $S \to \infty$ then $\vartheta_T(3\tau_b) = \vartheta_B(3\tau_b) = 7\vartheta_{\max}/4$.

We therefore conclude that at the end of the procedure, i.e. at $t = \tau_a$ , if $\nu$ heartbeats have occurred in the whole application time $\tau_a$, the tissue temperature is between $\nu\vartheta_{\max}$ and a lower value, say $\alpha\nu\vartheta_{\max}$ with $\alpha < 1$, which can be calculated by repeating the procedure just described and letting $S \to \infty$. It is therefore crucial to estimate the value of $S$ as the following scenario could occur: $\nu\vartheta_{\max}$ corresponds to a temperature that could potentially damage the area surrounding the application spot (including the esophagus) while $\alpha\nu\vartheta_{\max}$ may correspond to a safe temperature. In this case, of course, the model can provide useful indications only if a reliable estimate of $S$ is available. In the Appendix, we find that a reliable estimate of $S$ is $\approx 10^3$ ($\mathrm{Js^{-1}m^{-2}K^{-1}}$). Fig. 6 shows the behavior of $\vartheta_T(3\tau_b)$ for $t_p \in (10^{-4}\mathrm{s}, 10^{-3}\mathrm{s})$ for three values of $S$. It should be noticed that the tissue temperature can reach considerably high values above the basal one.

## 5. Solid tissue and blood temperature evolution during the diffusion stage

At the end of the first application, i.e. at $t = \tau_a$, the tissue hemisphere has temperature $\vartheta_T(\tau_a)$, which may range from $\nu\vartheta_{\max}$ and $\alpha\nu\vartheta_{\max}$, depending on $S$. We now consider the case in which there are three hot spots (that is, three points where the heating device touches the tissue, see Fig. 7. Investigating a worst case scenario, we assume that the esophagus wall is parallel to the $x$−axis of Fig. 7, and approximate the ostium to a plane. If $2h$ is the typical distance between the ostium and the esophagus, then the three hemispheres shown in Fig. 7 schematize the regions where heat is generated (because the current flows through them) that are close to the esophagus.

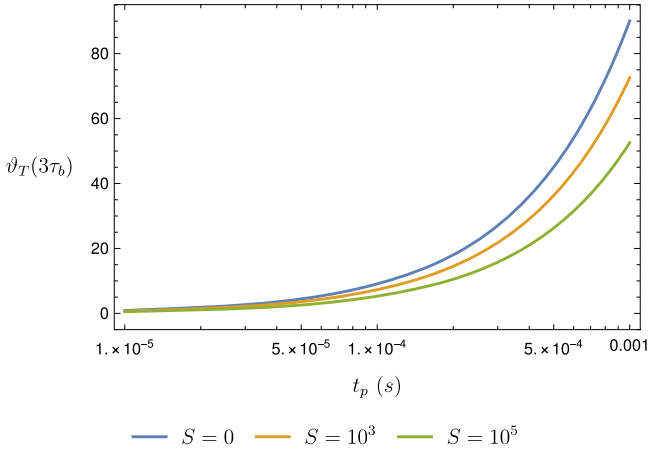


**Fig. 6.** $\vartheta_T(3\tau_b)$ for $t_p \in (10^{-5}s, 10^{-3}s)$, and for three values of $S$. The plot seems to indicate that the crucial role to operate safely is played by $t_p$ rather than by $S$.

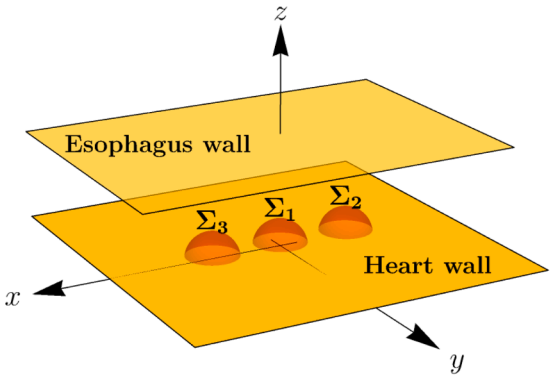


**Fig. 7.** Three hot spots of the device touch the pericardium. The integration region of system (13) is $z > 0$ (tissue side).

So, rescaling to 0 the time $t$, we have this parabolic problem

$$\begin{cases} \varrho c \dfrac{\partial \vartheta_T}{\partial t} = k\Delta\vartheta_T, & x, y \in \mathbb{R},\ z > 0,\ \ t > \tau_a, \\ \vartheta_T(\boldsymbol{X}, \tau_a) = \vartheta_T(\tau_a)\chi(\Sigma), & \boldsymbol{X} \in \mathbb{R}^3 \\ \vartheta_T(\boldsymbol{X}, t)|_{z=0} = 0, & \boldsymbol{X} \in \mathbb{R}^3 \end{cases} \tag{13}$$

where $\boldsymbol{X} = (x, y, z)$ is the position vector, $\chi(\Sigma)$ denotes the characteristic function of the region

$$\Sigma = \Sigma_1 \cup \Sigma_2 \cup \Sigma_3,$$

where

$$\Sigma_1 = \left\{\boldsymbol{X} \in R^3 :\ |\boldsymbol{X} - \boldsymbol{C}_1| \le h/2,\ z > 0\right\},$$
$$\Sigma_2 = \left\{\boldsymbol{X} \in R^3 :\ |\boldsymbol{X} - \boldsymbol{C}_2| \le h/2,\ z > 0\right\},$$
$$\Sigma_3 = \left\{\boldsymbol{X} \in R^3 :\ |\boldsymbol{X} - \boldsymbol{C}_3| \le h/2,\ z > 0\right\},$$

and

$$\boldsymbol{C}_1 = (0, 0, 0), \qquad \boldsymbol{C}_2 = (-2h, 0, 0), \qquad \boldsymbol{C}_3 = (2h, 0, 0).$$

The boundary condition at $z = 0$ is justified by the fact that the tissue is in contact with the blood at basal temperature.

During a standard PFA procedure, $\mathcal{N}_{\text{app}}$ consecutive applications are delivered, in which the contact points with the ostium vary. Specifically, after each application (lasting $\tau_a$), the device is rotated before delivering the next application. Thus, $\mathcal{N}_{\text{app}}$ applications are performed, each separated by a time interval $\Delta$. This creates alternating heating and cooling (diffusion) phases, leading to a cumulative thermal effect. To be precise, each time the device touches the inner wall of the PV ostium, heat is transferred to the tissue, leading to localized temperature rise. Between pulses, heat diffuses into surrounding tissues. Clearly, the depth and extent of heating depend not only on the thermal properties of the surrounding tissues but also on the heat source intensity and the number of applications. Due to the linearity of the heat equation, the temperature evolution in the tissue can be computed as the superposition of $\mathcal{N}_{\text{app}}$ solutions to problem (13), assuming an initial temperature of $\vartheta(\tau_a)\chi(\Sigma)$. In other words, if $\Delta$ is the time lapse separating two subsequent heating phases, and $\vartheta(t)$ is the solution of system (13) (first diffusion stage), the whole evolution after $\mathcal{N}_{\text{app}}$ applications, is given by

$$\Theta(t) = \sum_{i=0}^{\mathcal{N}_{\text{app}}} \mathcal{H}(t - i\Delta)\vartheta(t - i\Delta), \tag{14}$$

where $\mathcal{H}$ is the Heaviside function. In our approach the intensity of thermal effects is directly linked to the choice of $t_p$ (time duration of the electrical pulse), $S$ (the heat transfer coefficient at the blood-tissue interface), and $\mathcal{N}_{\text{app}}$ (number or repeated application).

We consider three cases: $t_p = 2 \times 10^{-4}$s, $t_p = 10^{-4}$s, and $t_p = 8 \times 10^{-5}$s. In all cases, we fix $\mathcal{N}_{\text{app}} = 8$, $S = 10^3\,\text{Js}^{-1}\text{m}^{-2}\text{K}^{-1}$, (we will discuss the reason of this choice in the A). Fig. 8 shows the evolution of $\vartheta$ at $(0, 0, 2h)$ that may correspond to the esophagus lumen during the whole process when the applied voltage is $2 \times 10^3$V (values of this order of magnitude have been reported in Verma et al., 2022; Lemoine et al., 2023).

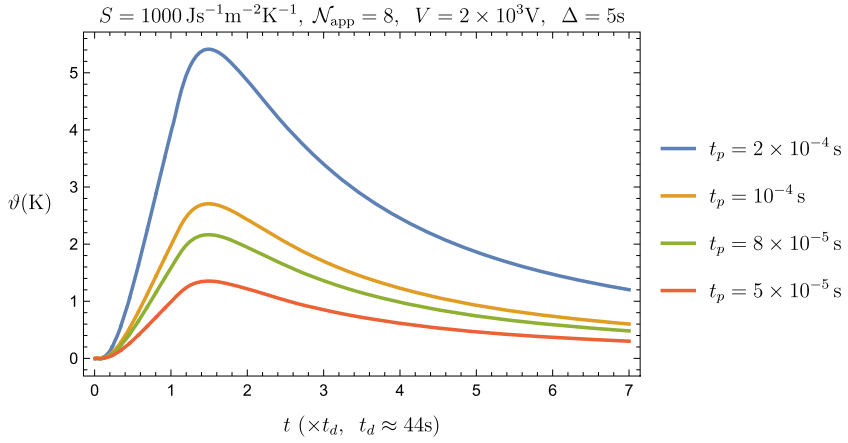


**Fig. 8.** Evolution of the thermal field generated by three hot spots at the esophagus wall ($2h$ from the interface) when $t_p = 2 \times 10^{-4}$s, $t_p = 10^{-4}$s, $t_p = 8 \times 10^{-5}$s, and $t_p = 5 \times 10^{-5}$s when $S = 10^3\text{Js}^{-1}\text{m}^{-2}\text{K}^{-1}$, $\mathcal{N}_{\text{app}} = 8$, and $\Delta = 5$s. We recall that $t_d \approx 44$ (s), so that the time interval represented in the graph is about 5 min. The applied voltage is $2 \times 10^3$V.

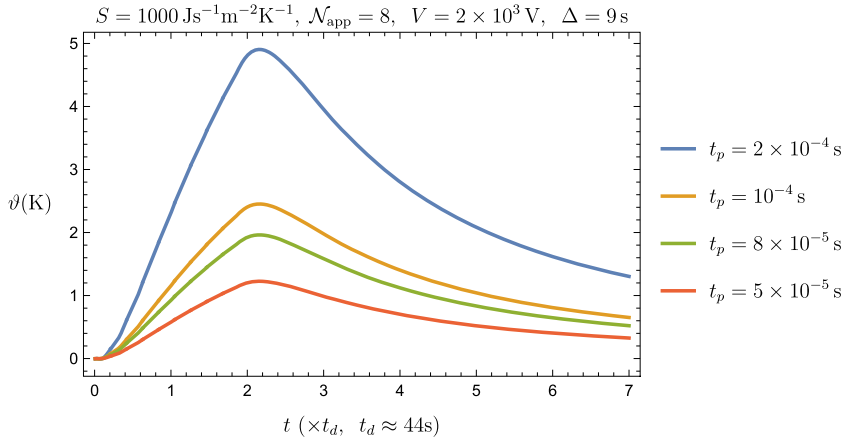


**Fig. 9.** Evolution of the thermal field generated by three hot spots at the esophagus distance ($2h$ from the interface) when $t_p = 2 \times 10^{-4}$s, $t_p = 10^{-4}$s, $t_p = 8 \times 10^{-5}$s, and $t_p = 5 \times 10^{-5}$s when $S = 10^3\text{Js}^{-1}\text{m}^{-2}\text{K}^{-1}$, $\mathcal{N}_{\text{app}} = 8$, and $\Delta = 9$s. We recall that $t_d \approx 44$ (s), so that the time interval represented in the graph is about 5 min. The applied voltage is $2 \times 10^3$V.

**Table**
List of symbols (denoting both variables and constants) used throughout the paper. Here, only SI units are indicated although, occasionally, various alternative units or sub-units are used.

| Symbol | Unit | Meaning | Typical value |
|---|---|---|---|
| $\vartheta_B$ | K | blood temperature (respect to basal one) | $\approx 1-2$ |
| $\vartheta_T$ | K | tissue temperature (respect to basal one) | $\approx 1-5$ |
| $\sigma$ | $\Omega^{-1}m^{-1}$ | electric conductivity | 1 |
| $S$ | $Js^{-1}m^{-2}K^{-1}$ | heat transfer coefficient | $10^3$ |
| $\varrho$ | $Kgm^{-3}$ | density | $1.5\times10^3$ |
| $c$ | $JKg^{-1}K^{-1}$ | heat capacity | $3.7\times10^3$ |
| $k$ | $Js^{-1}m^{-1}K^{-1}$ | heat conductivity | 0.5 |
| $\tau_p$ | s | pulse period | 0.5 |
| $\tau_a$ | s | application time | 2.5 |
| $\tau_b$ | s | blood replacement time | 1 |
| $t_p$ | s | high voltage application time | $\approx 10^{-4}$ |
| $t_w$ (see (5)) | s | heating time | $\approx 10^{-5}$ |
| $t_d$ (see (6)) | s | diffusion time | $\approx 10$ |
| $h$ | m | characteristic length | $2\times10^{-3}$ |
| $Z$ (see (3)) | $\Omega$ | electric resistance | $\approx 10^3$ |
| $V$ | V | applied tension | $2\times10^3$ |
| $V_{el}$ | $m^3$ | element volume | $\approx 10^{-8}$d |
| $W$ (see (4)) | $Js^{-1}$ | dissipated power | $\approx 10^3$ |
| $a^2$ (see (A.2)) | $m^{-2}s^{-1}$ | thermal diffusivity | $\approx 10^{-2}$ |

We can clearly see that, the cases $t_p = 2\times10^{-4}$s depicts a potentially dangerous situation. Particularly alarming is the fact that for $t_p = 2\times10^{-4}$s the permanence time of the esophageal temperature at values exceeding the basal temperature by more than 4K is estimated to be more than a minute (and by more than 3K about two minutes). This might be enough to produce serious lesions. Of course we remind that these results refer to a worst case situation (esophagus close to the ablation site, long pulses duration), they do not mean that PFA is necessarily dangerous but they just provide a theoretical explanation of the event reported in Kirstein et al. (2024). Obviously the outcome is even worse if we consider pulses of larger amplitude.

Fig. 9 shows the temperature evolution in a similar setting still assuming the applied voltage to be $2\times10^3$V but increasing $\Delta$ to 9s. Also in that case the temperature increase (and the permanence time above 4K) looks quite alarming unless $t_p$ remains below $10^2$ microseconds.

## 6. Conclusions

As far we are aware, aside from the study by Kirstein et al. (2024), there are no experimental data on the thermal effects of PFA. Our paper aims to highlight this relatively unexplored topic by investigating the thermal dynamics of PFA. We have formulated a mathematical model to investigate the thermal field generated during successive applications of pulsed field ablation. The aim was to understand to what extent the claim that PFA is a non-thermal procedure is acceptable, since at least one case of non-negligible increase of the luminal esophageal temperature has been reported (Kirstein et al., 2024). The crucial point in this analysis is the distinction of the time scales involved and in particular the fact that diffusion time is much larger than the heating time of the ablation spots. This allowed to compute the temperature at the esophagus location through a two-step calculation, introducing some simplification in the geometry of the considered domain. It turns out that in this respect the most important parameter of the procedure is the duration time of the electric pulse, since the predicted increment of the luminal esophageal temperature (when the esophagus is critically close to the atrium) can be of several degrees when the pulse duration is $10^{-3}$s. However, even when the pulse duration is on the order of $10^{-4}$s, the model predicts that the luminal esophageal temperature could remain above critical levels for one to two minutes, an outcome that presents a potentially unsafe scenario. We believe this indication can be of some importance for the users, letting them be aware that choosing extreme values of the emitted electric pulses may result in sizable and dangerous heating of neighboring organs.

## CRediT authorship contribution statement

**Angiolo Farina:** Writing – original draft, Supervision, Formal analysis, Conceptualization; **Antonio Fasano:** Writing – review & editing, Writing – original draft, Supervision, Investigation, Formal analysis, Conceptualization; **Massimo Grimaldi:** Writing – review & editing, Supervision, Methodology, Investigation, Conceptualization; **Fabio Rosso:** Writing – review & editing, Writing – original draft, Supervision, Software, Investigation, Formal analysis, Conceptualization.

## Declaration of competing interest

The authors declare that they have no known competing financial interests or personal relationships that could have appeared to influence the work reported in this paper.

## Appendix A. Estimating the heat exchange coefficient $S$

In the present section we examine the heat equation within the finite layer $(-h, h)$, assuming zero heat flux at the boundaries and a temperature jump at $x = 0$ and $t = 0$. We rescale the spatial variable to $(0, 1)$ and the temperature with its initial value, i.e.

$$y = \frac{1}{2h}(h + x), \qquad u = \frac{\vartheta}{\vartheta_o}$$

to get

$$\begin{cases} u_t - a^2 u_{xx} = 0, & y \in (0,1), \quad t \geq 0, \\ u(x,0) = u_o f(y), & y \in (0,1) \\ u_x(0,t) = u_x(1,t) = 0 & t \geq 0, \end{cases} \tag{A.1}$$

where

$$a^2 = \frac{k}{4h^2 \varrho c}, \tag{A.2}$$

and

$$f(y) = \begin{cases} 0, & \text{if } y \in (0, 1/2) \\ 1 & \text{if } y \in (1/2, 1). \end{cases}$$

The solution of problem (A.1), is the sum of an infinite series, namely (see, e.g. Tikhonov and Samarskii, 2013)

$$u(y,t) = \frac{a_o}{2} + \sum_{n=1}^{+\infty} a_n \exp(-\pi^2 a^2 n^2 t)\cos(n\pi y), \tag{A.3}$$

where

$$a_n = 2\int_0^1 f(y)\cos(n\pi y)\,dy = 2\int_{1/2}^1 \cos(n\pi y)\,dy, \qquad n \geq 0,$$

that is

$$a_o = 1, \qquad a_n = -\frac{2}{n\pi}\sin\left(\frac{n\pi}{2}\right), \text{for } n \geq 1.$$

Evaluating the heat flux at $y = 1/2$ we get

$$J(t) = -k\frac{\vartheta_o}{2h}u_y(1/2,t) = -k\frac{\vartheta_o}{h}\sum_{n=1}^{+\infty}\sin^2(n\pi/2)\exp\left(-\pi^2 a^2 n^2 t\right). \tag{A.4}$$

Finally, the amount of heat transmitted through $y = 1/2$ (which corresponds to $x = 0$) during the time interval $(0, \tau_B)$ is (after some algebra)

$$Q = \int_0^{\tau_B} |J(t)\,dt| = \frac{4\varrho c h}{\pi^2}\vartheta_o \sum_{n=1}^{+\infty}\frac{\sin^2(n\pi/2)}{n^2}\left[1 - \exp(-\pi^2 a^2 n^2 \tau_B)\right]. \tag{A.5}$$

It is worth noticing that, as $\tau_B \to \infty$, $Q \to \varrho c h \vartheta_o/2$ as it to be expected just on the base of elementary physics.

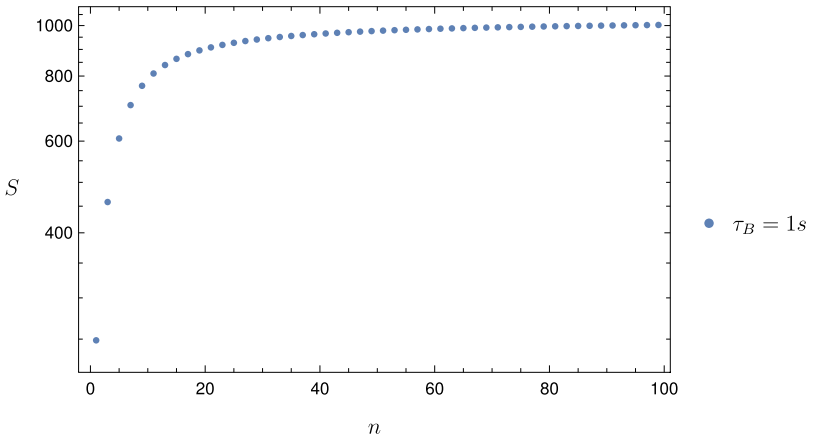


**Fig. A.1.** Estimate of the heat exchange coefficient $S$.

We now recall the approach based on the evaluation of the average temperatures $\vartheta_t, \vartheta_b$ on the intervals $(-h, 0)$ and $/0, h)$, respectively, which makes use of the parameter $S$:

$$\begin{cases} h\varrho c\ \dfrac{d\hat{\vartheta}_b}{dt} = S\left(\hat{\vartheta}_t - \hat{\vartheta}_b\right), \\ h\varrho c\ \dfrac{d\hat{\vartheta}_t}{dt} = -S\left(\hat{\vartheta}_t - \hat{\vartheta}_b\right), \\ \hat{\vartheta}_t(0) = \vartheta_o, \quad \hat{\vartheta}_b(0) = 0. \end{cases} \tag{A.6}$$

whose solution is

$$\hat{\vartheta}_t(S) = \frac{\vartheta_o}{2}\left[1 + \exp\left(-\frac{2S}{\varrho c h}\right)\right], \quad \hat{\vartheta}_b(S) = \frac{\vartheta_o}{2}\left[1 - \exp\left(-\frac{2S}{\varrho c h}\right)\right]. \tag{A.7}$$

Using (A.7), the heat flux (per unit surface and unit time) which is exchanged between the blood and the tissue is

$$J(S,t) = S(\hat{\vartheta}_b - \hat{\vartheta}_t) = -S\vartheta_o \exp\left(-\frac{2S}{\varrho c h}t\right) \tag{A.8}$$

and the total heat exchanged after $\tau_B$ units of time is

$$Q(S) = \int_0^{\tau_B} |J(t)|\, dt = \frac{\varrho c h}{2}\vartheta_o\left[1 - \exp\left(-\frac{2S}{\varrho c h}\tau_B\right)\right] \tag{A.9}$$

We recall that (A.9) represents a reasonable approximation of total heat exchanged, while the exact value is provided by (A.5). By comparing the two expressions, we get

$$S = -\frac{\varrho c h}{2\tau_B}\ln\left\{1 - \frac{8}{\pi^2}\sum_{n=1}^{+\infty}\frac{\sin^2(n\pi/2)}{n^2}\left[1 - \exp\left(-\pi^2\frac{k}{4h^2\varrho c}n^2\tau_B\right)\right]\right\}.$$

Fig. A.1 illustrates the estimate of $S$ for $\tau_B = 1$ s computed using a sufficiently large number of terms in the series.

To complete this analysis, let us define $x = s(t)$ the position along $x > 0$ where $\vartheta(s(t), t) = 10^{-2}\vartheta_o$. This definition allows us to calculate the time required for $s(t)$ to reach the distance $h$. Since

$$\vartheta(s(t), t) = \vartheta_o\left[1 - \mathrm{erf}\left(\frac{s(t)\sqrt{\varrho c}}{\sqrt{kt}}\right)\right],$$

and $1 - \mathrm{erf}(\xi) = 0.01$ for $\xi \simeq 1.8$, we get

$$s(t) \simeq 3\sqrt{\frac{k}{\varrho c}t}.$$

For $h = 2$mm and the already given values of $\varrho, c, k$, we find $t \simeq 4$s. Specifically, if $\tau_B = 1$s, the initial temperature at $x = h/4$ decreases to 1 % of $\vartheta_o$ (i.e. 0.3K if $\vartheta_o = 30$K). This implies that, within a single application lasting approximately 3s the amount of heat reaching $x = h$ is negligible.

## References


Badertscher, P., Knecht, S., Rosso, R., Krisai, P., Spreen, D., Katic, J., de Lavallaz, J. D.F., Sticherling, C., Kühne, M., 2025. How to perform pulmonary vein isolation using a pentaspline pulsed field ablation system for treatment of atrial fibrillation. Heart Rhythm 22 (1), 69–79.

Cho, M.S., Lee, S.-R., Black-Maier, E., Jackson, K.P., Friedman, D.J., Pokorney, S.D., Loring, Z., Febre, J., Piccini, J.P., 2024. Complications associated with pulsed field ablation vs radiofrequency catheter ablation of atrial fibrillation. Heart Rhythm https://doi.org/10.1016/j.hrthm.2024.10.063.

de Asmundis, C., Chierchia, G.-B., 2021. Pulsed field ablation: have we finally found the holy grail? EP Europace 23 (11), 1691–1692.

Deering, T.F., Bunch, T.J., Lakkireddy, D., Liu, C.F., Piccini, J.P., Smith, A.M., 2024. Pulsed field ablation: a promise with future broad-based applicability or a pause needing further analysis-is catheter ablation at a crossroads? A critical appraisal of the new challenger-pulsed field ablation. Heart Rhythm 21 (8), 1242–1244.

Farina, A., Fasano, A., Rosso, F., 2024. Modeling thermal effects of pulsating currents in human tissues: how to prevent necrosis. Biophysica 4 (4), 477–487.

Farnir, F., Chaldoupi, S.-M., Hermans, B. J.M., Farnir, F., Habibi, Z., Jerltorp, K., Verhaert, D., Schotten, U., Maesen, B., Vernooy, K., et al., 2025. A tailored substrate-based approach using focal pulsed field catheter ablation in patients with atrial fibrillation and advanced atrial substrate: procedural data and 6-months success rates. Heart Rhythm https://doi.org/10.1016/j.hrthm.2025.01.015.

Grimaldi, M., Di Monaco, A., Gomez, T., Berman, D., Datta, K., Sharma, T., Govari, A., Altmann, A., Di Biase, L., 2022. Time course of irreversible electroporation lesion development through short-and long-term follow-up in pulsed-field ablation–treated hearts. Circ. Arrhythmia Electrophysiol. 15 (7), e010661.

Kirstein, B., Heeger, C.-H., Vogler, J., Eitel, C., Feher, M., Phan, H.-L., Mushfiq, I., Traub, A., Hatahet, S., Samara, O., et al., 2024. Impact of pulsed field ablation on intraluminal esophageal temperature. J. Cardiovasc. Electrophysiol. 35 (1), 78–85.

Kocharian, A.A., Murthy, M.K., Patel, A., Venkataraman, R., Mathuria, N.S., Lador, A., Fahed, J., Valderrábano, M., 2025. Luminal esophageal temperature rises with pulsed field ablation. Clin. Electrophysiol. https://doi.org/10.1016/j.jacep.2025.02.037.

Lemoine, M.D., Fink, T., Mencke, C., Schleberger, R., My, I., Obergassel, J., Bergau, L., Sciacca, V., Rottner, L., Moser, J., et al., 2023. Pulsed-field ablation-based pulmonary vein isolation: acute safety, efficacy and short-term follow-up in a multi-center real world scenario. Clin. Res. Cardiol. 112 (6), 795–806.

Pearce, J.A., 2013. Comparative analysis of mathematical models of cell death and thermal damage processes. Int. J. Hyperthermia 29 (4), 262–280.

Peters, J., Stinstra, G., Hendriks, M., 2001. Estimation of the electrical conductivity of human tissue. Electromagnetics 21 (7–8), 545–557.

Rattka, M., Mavrakis, E., Vlachopoulou, D., Rudolph, I., Kohn, C., Bohnen, J., Yahsaly, L., Siebermair, J., Wakili, R., Jungen, C., et al., 2024. Pulsed field ablation and cryoballoon ablation for pulmonary vein isolation: insights on efficacy, safety and cardiac function. J. Interventional Card. Electrophysiol. 67 (5), 1191–1198.

Reddy, V.Y., Neuzil, P., Koruth, J.S., Petru, J., Funosako, M., Cochet, H., Sediva, L., Chovanec, M., Dukkipati, S.R., Jais, P., 2019. Pulsed field ablation for pulmonary vein isolation in atrial fibrillation. J. Am. Coll. Cardiol. 74 (3), 315–326.

Shehadeh, M., Wan, E.Y., Biviano, A., Mollazadeh, R., Garan, H., Yarmohammadi, H., 2024. Esophageal injury, perforation, and fistula formation following atrial fibrillation ablation. J. Interventional Card. Electrophysiol. 67 (2), 409–424.

Tang, J.E., Guirguis, F., Stein, E.J., Essandoh, M.K., Iyer, M.H., 2024. Pulse field ablation: the electric future of cardiac ablation. J. Cardiothorac. Vasc. Anesth. 38 (10), 2139–2142.

Tikhonov, A.N., Samarskii, A.A., 2013. Equations of Mathematical Physics. Courier Corporation.

Verma, A., Boersma, L., Haines, D.E., Natale, A., Marchlinski, F.E., Sanders, P., Calkins, H., Packer, D.L., Hummel, J., Onal, B., Rosen, S., Kuck, K.-H., Hindricks, G., Wilsmore, B., 2022. First-in-human experience and acute procedural outcomes using a novel pulsed field ablation system: the PULSED AF pilot trial. Circ. Arrhythmia Electrophysiol. 15 (1), e010168.

Yoo, D.H., Heist, E.K., 2024. Pulsed field ablation for atrial fibrillation: is it truly as good as it sounds? J. Interventional Card. Electrophysiol. 67 (2), 237–238.